**The EMBO Journal** Vol. 22 No. 7 pp. 1478–1487, 2003

# Functional expression of the epithelial $Ca^{2+}$ channels (TRPV5 and TRPV6) requires association of the S100A10–annexin 2 complex

**Stan F.J.van de Graaf, Joost G.J.Hoenderop, Dimitra Gkika, Dennis Lamers, Jean Prenen[1], Ursula Rescher[2], Volker Gerke[2], Olivier Staub[3], Bernd Nilius[1] and René J.M.Bindels[4]**

Department of Cell Physiology, Nijmegen Center for Molecular Life Sciences, University Medical Center Nijmegen, PO Box 9101, NL-6500 HB Nijmegen, The Netherlands, [1]Department of Physiology, Campus Gasthuisberg, KU Leuven, B-3000 Leuven, Belgium, [2]Institute of Medical Biochemistry, University of Münster, von-Esmarch-strasse 56, D-48149 Münster, Germany and [3]Institute of Pharmacology and Toxicology, University of Lausanne, CH-1005 Lausanne, Switzerland

[4]Corresponding author
e-mail: r.bindels@ncmls.kun.nl

**TRPV5 and TRPV6 constitute the $Ca^{2+}$ influx pathway in a variety of epithelial cells. Here, we identified S100A10 as the first auxiliary protein of these epithelial $Ca^{2+}$ channels using yeast two-hybrid and GST pull-down assays. This S100 protein forms a heterotetrameric complex with annexin 2 and associates specifically with the conserved sequence VATTV located in the C-terminal tail of TRPV5 and TRPV6. Of these five amino acids, the first threonine plays a crucial role since the corresponding mutants (TRPV5 T599A and TRPV6 T600A) exhibited a diminished capacity to bind S100A10, were redistributed to a subplasma membrane area and did not display channel activity. Using GST pull-down and co-immunoprecipitation assays we demonstrated that annexin 2 is part of the TRPV5–S100A10 complex. Furthermore, the S100A10–annexin 2 pair colocalizes with the $Ca^{2+}$ channels in TRPV5-expressing renal tubules and TRPV6-expressing duodenal cells. Importantly, down-regulation of annexin 2 using annexin 2-specific small interfering RNA inhibited TRPV5 and TRPV6-mediated currents in transfected HEK293 cells. In conclusion, the S100A10–annexin 2 complex plays a crucial role in routing of TRPV5 and TRPV6 to plasma membrane.**

*Keywords*: CaT1/ECaC/p11/PDZ motif/siRNA

## Introduction

The epithelial $Ca^{2+}$ channels TRPV5 and TRPV6 (recently renamed after ECaC1 and ECaC2, respectively) belong to the superfamily of transient receptor potential (TRP) channels (Montell *et al*., 2002a,b). The physiological function of this group of non-selective cation channels is diverse and ranges from involvement in phototransduction, olfaction, nociception, sexual behavior, heat and cold sensation, to epithelial $Ca^{2+}$ transport (Montell *et al*., 2002a). Moreover, these channels display a plurality in ion selectivities and activation mechanisms, some of which represent previously unrecognized modes of channel regulation (Montell *et al*., 2002a).

TRPV5 and TRPV6 are by far the most $Ca^{2+}$-selective channels of the TRP superfamily and constitute the rate-limiting influx step in active $Ca^{2+}$ (re)absorption that takes place in kidney, proximal intestine and placenta (Hoenderop *et al*., 2001b, 2002b). A delicate regulation of their activity is of utmost importance to maintain the extracellular $Ca^{2+}$ balance. Several lines of evidence demonstrate that these $Ca^{2+}$ channels are, indeed, controlled by various mechanisms (Hoenderop *et al*., 2002b). First, TRPV5 and TRPV6 display a $Ca^{2+}$-dependent feedback regulation of channel activity. The intracellular $Ca^{2+}$ concentration in close proximity to the channel mouth exerts an inhibitory effect on channel activity. Several domains in the channel protein sequence have been implicated in this inhibitory mechanism (Nilius *et al*., 2002). Secondly, the recovery from the $Ca^{2+}$-dependent inactivation renders another plausible site of regulation. This recovery is a relatively slow process that may reflect an intrinsic property of TRPV5 and TRPV6 or could result from (re)insertion of channels from an intracellular pool (Vennekens *et al*., 2000; Nilius *et al*., 2001). A significant subset of TRPV5 channels is localized subapically in distal tubules of the kidney, hinting at a shuttling mechanism of these channels to the plasma membrane (Loffing *et al*., 2001). Thirdly, vitamin D, estrogen and dietary $Ca^{2+}$ content have been shown to regulate the abundance of these $Ca^{2+}$ channels, resulting in normalization of hypocalcemia in 25-hydroxyvitamin $D_3$-1$\alpha$-hydroxylase (1$\alpha$-OHase) knockout mice (Hoenderop *et al*., 2001a, 2002a; Van Cromphaut *et al*., 2001; Van Abel *et al*., 2002). Fourthly, the amino acid sequence of TRPV5 and TRPV6 contains conserved motifs for putative regulatory activities including protein kinase C phosphorylation sites, ankyrin repeats and PDZ motifs (Hoenderop *et al*., 2001b). To date, little information is available concerning the molecular players responsible for these processes regulating the activity of TRPV5 and TRPV6. A number of regulatory proteins have recently been described that modify the biophysical, pharmacological and expression properties of ion channels and transporters by direct interactions (Li and Montell, 2000; Liedtke *et al*., 2000). These newly identified associated proteins have facilitated the elucidation of important molecular pathways modulating transport activity.

The aim of the present study was, therefore, to identify auxiliary proteins interacting specifically with TRPV5 and TRPV6. To this end, we have used a yeast two-hybrid screen to identify proteins associated with the epithelial $Ca^{2+}$ channels. The functional interaction between TRPV5

and TRPV6 and the identified interacting protein was further substantiated by pull-down assays, immunohistological studies, RNA interference (RNAi) and electrophysiological analysis of the regulatory effect of the newly identified protein ligands on TRPV5 and TRPV6 activity.

## Results

### *Identification of S100A10 as TRPV5-associated protein*

To identify proteins that interact with TRPV5, the C-terminal tail of TRPV5 was used to screen a mouse kidney cDNA library using the yeast two-hybrid technique. One of the positive clones encoded S100A10, a distinct member of the EF-hand-containing S100 protein family. S100A10 is also known as calpactin light chain, p11 or annexin 2 light chain (Rety *et al*., 1999). To confirm this interaction, the full-length S100A10 coding sequence was analyzed with the C-terminal tail of TRPV5 as bait using the yeast two-hybrid system (Figure 1A). As a negative control the γ subunit of the epithelial $Na^+$ channel, γENaC, was used. S100A10 strongly interacted with TRPV5, whereas no binding was observed with γENaC, indicating the specificity of the S100A10–TRPV5 interaction (Figure 1B). In addition, β-galactosidase activity was not detectable in the absence of prey, or after co-transformation of the bait with the empty pACT2 (prey) vector (data not shown).

### *S100A10 interacts with TRPV5 and TRPV6*

To further establish the interaction between TRPV5 and S100A10, GST pull-down binding assays were performed. *Xenopus laevis* oocytes were injected with S100A10 cRNA and homogenized after 3 days. The S100A10-containing homogenate was incubated with GST or GST–TRPV5 fusion proteins immobilized on glutathione–Sepharose 4B beads. S100A10 bound specifically to the C-terminal tail of TRPV5, since no interaction was observed with GST alone (Figure 1C). Subsequently, this binding was investigated in the presence of 1 mM $Ca^{2+}$ or 2 mM EDTA as shown in Figure 1D. S100A10 interacted with the C-terminal tail of TRPV5 in a $Ca^{2+}$-independent manner. In addition, [$^{35}$S]methionine-labeled full-length TRPV5 protein bound to GST–S100A10, whereas GST alone was negative (Figure 1E). Interestingly, the interaction with S100A10 was not restricted to TRPV5, since S100A10 also interacted with the C-terminal tail of TRPV6 (Figure 1C). Likewise, [$^{35}$S]methionine-labeled full-length TRPV6 bound to S100A10 immobilized on glutathione–Sepharose 4B beads, confirming the TRPV6–S100A10 interaction (Figure 1E).

### *TRPV5 interacts with the S100A10–annexin 2 complex*

S100A10 forms a heterotetramer with annexin 2, which is a member of the $Ca^{2+}$ and phospholipid binding proteins (Gerke and Moss, 2002). This heterotetramer consists of a S100A10 dimer binding to two annexin 2 molecules in a highly symmetrical manner (Rety *et al*., 1999). In *X.laevis* oocytes S100A10 also forms a dimer, as was demonstrated by chemical cross-linking using dimethyl-3′-3′-dithiobispropionimidate·2HCl (DTBP) in S100A10 cRNA injected oocytes (Figure 2A). To demonstrate the presence of

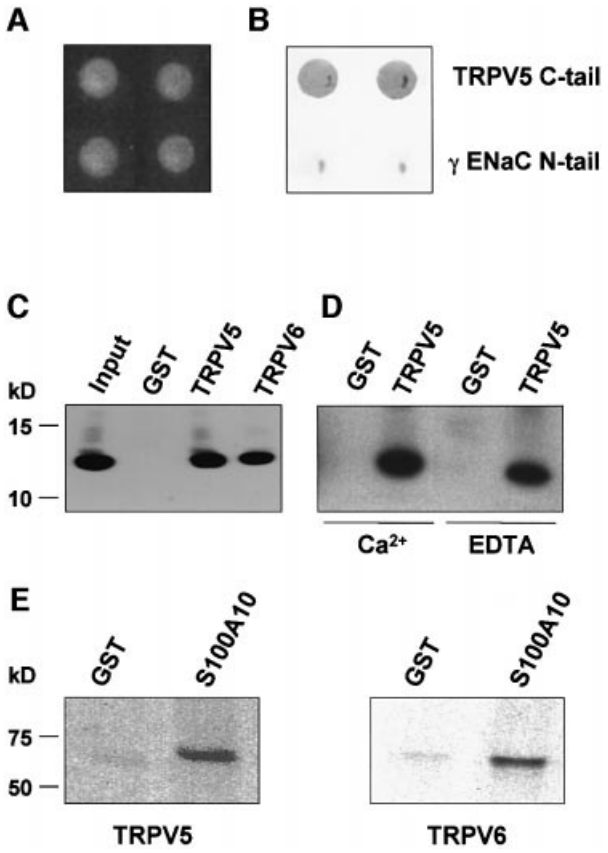


**Fig. 1.** Interaction of TRPV5 and S100A10 as shown by yeast two-hybrid and GST pull-down analyses. (**A**) The C-terminal tail of TRPV5 or γENaC and full-length S100A10 were cotransformed into the Y153 yeast strain and grown on media without tryptophan and leucine. (**B**) β-galactosidase activity was demonstrated in TRPV5 and S100A10 cotransformed yeast, whereas no activity was observed in γENaC and S100A10 cotransformed yeast. Two representative colonies are depicted. (**C**) Lysates of *X.laevis* oocytes injected with 20 ng of VSV-tagged S100A10 cRNA were incubated with GST or GST fused to the C-terminal tail of TRPV5 or TRPV6 immobilized on glutathione–Sepharose 4B beads. S100A10 interacted specifically with TRPV5 and TRPV6, but not with GST alone. (**D**) The experiment was performed as outlined in (C). Binding of S100A10 to TRPV5 was demonstrated in the presence of 1 mM $Ca^{2+}$ or 2 mM EDTA. (**E**) [$^{35}$S]methionine-labeled full-length TRPV5 or TRPV6 was incubated with GST or GST–S100A10 immobilized on glutathione–Sepharose 4B beads. Both TRPV5 and TRPV6 interacted with S100A10, whereas no binding to GST alone was observed.

annexin 2 in the S100A10–TRPV5 complex, GST pull-down assays and co-immunoprecipitations of these proteins in their native form were performed. To this end, annexin 2 and a vesicular stomatitis virus glycoprotein (VSV)-tagged S100A10 cRNA were co-injected in *X.laevis* oocytes. Subsequently, these oocytes were metabolically labeled with [$^{35}$S]methionine and homogenized in pull-down buffer containing 2 mM EDTA. Solubilized proteins were immunoprecipitated using anti-VSV antibodies. Annexin 2 could be co-immunoprecipitated with S100A10, demonstrating the presence of an S100A10–annexin 2 complex in these oocytes (Figure 2A). In addition, annexin 2 was precipitated from homogenates of S100A10–annexin 2 cRNA co-injected oocytes using GST–TRPV5 C-terminal tail-loaded glutathione–Sepharose 4B beads (Figure 2B), demonstrating a physical interaction between TRPV5, S100A10 and annexin 2.

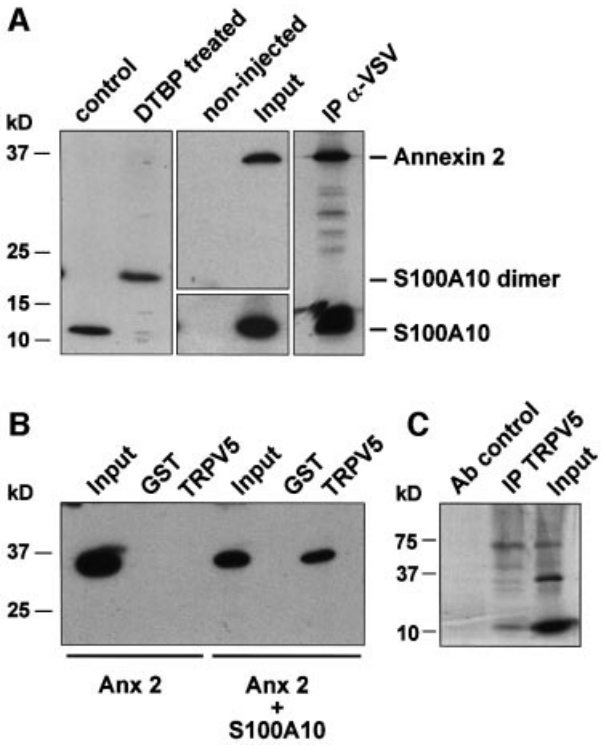


**Fig. 2.** Annexin 2 interacts with TRPV5 via S100A10. *Xenopus laevis* oocytes were injected with S100A10 or co-injected with annexin 2 and VSV-tagged S100A10 cRNAs. (**A**) Lysates of S100A10 cRNA-injected oocytes were treated with DTBP and analyzed by immunoblot. The chemically cross-linked S100A10 band runs at 23 kDa, exactly the expected size of a VSV-tagged S100A10 dimer. Homogenates of non-injected and oocytes co-injected with S100A10 and annexin 2 cRNAs were subjected to immunoprecipitation using monoclonal anti-VSV antibodies. Annexin 2 co-immunoprecipitated with S100A10 as was visualized by autoradiography of the metabolically labeled proteins. As a control, the expression of S100A10 and annexin 2 in the co-injected oocytes was demonstrated by immunoblot analysis to demonstrate that the precipitated proteins were of the correct size. (**B**) Homogenates of annexin 2 cRNA-injected or S100A10 and annexin 2 cRNA-co-injected oocytes were incubated with GST alone or GST fusion protein containing the TRPV5 C-terminal tail immobilized on glutathione–Sepharose 4B beads. The association of annexin 2 with TRPV5 in the presence of S100A10 was demonstrated by immunoblot using a monoclonal anti-annexin 2 antibody. (**C**) Full-length annexin 2, S100A10 and TRPV5 were *in vitro* translated using a reticulocyte lysate system in the presence of canine microsomal membranes. S100A10 and annexin 2 were co-immunoprecipitated with TRPV5 confirming the formation of a TRPV5–S100A10–annexin 2 complex.

However, the TRPV5–annexin 2 interaction could only be observed when S100A10 was co-expressed with annexin 2, indicating that S100A10 bridges annexin 2 to TRPV5. Finally, co-immunoprecipitations were performed using *in vitro*-translated TRPV5, S100A10 and annexin 2. S100A10 and annexin 2 co-immunoprecipitated with TRPV5, but not in a control reaction carried out with an unrelated antibody, confirming the specificity of the procedure (Figure 2C).

### *Co-localization of TRPV5, S100A10 and annexin 2 in $Ca^{2+}$-transporting epithelia*

Co-expression of S100A10 and annexin 2 in kidney and small intestine, which express TRPV5 and TRPV6 (Hoenderop *et al*., 1999a; Peng *et al*., 1999), was first investigated by RT–PCR. Using two specific primer sets a 239 and 360 bp product was amplified in kidney and duodenum, corresponding to the expected sizes of the S100A10 and annexin 2 fragments amplified. Subsequently, the cellular localization of these proteins was studied in kidney and duodenal sections by immunohistochemistry. In kidney, immunopositive staining for TRPV5 was predominantly present at the apical membrane of distal convoluted and connecting tubules (Figure 3A). S100A10 and annexin 2 co-localized with TRPV5, since an immunopositive staining for these proteins was observed along the apical domain of the TRPV5-expressing distal tubular cells. Importantly, the same observations were made for the localization of these proteins in duodenum, where TRPV6, S100A10 and annexin 2 were observed along the brush-border membrane (Figure 3B; for color images of this figure see the Supplementary data available at *The EMBO Journal* Online).

### *Mapping of the S100A10 binding site in TRPV5*

To identify the S100A10 binding site in TRPV5, a series of deletion mutants of the C-terminal tail of TRPV5 was constructed as shown in Figure 4. Truncated forms of TRPV5 were expressed as GST fusion proteins, and pull-down experiments were performed as described above. The interaction between S100A10 and TRPV5 was lost when TRPV5 was truncated at position 598, whereas truncations at positions 680 up to 603 had no effect on the interaction with S100A10. Subsequently, the identified S100A10 binding region between amino acids 598 and 603 (VATTV) was mutated into glycines, and the binding of S100A10 was analyzed by a GST pull-down assay. The binding between S100A10 and TRPV5 was virtually abolished when this putative binding region was mutated. Mutation of the first threonine in this motif into an alanine (TRPV5 T600A) also prevented the association of this protein, indicating the crucial role of this amino acid for binding of S100A10.

### *S100A10 binding to TRPV5 or TRPV6 is critical for channel activity*

The effect of S100A10 on TRPV5 and TRPV6 activity was determined by whole-cell patch–clamp analysis in transiently transfected human embryonic kidney (HEK293) cells, as shown in Figure 5A and B. HEK293 cells heterologously expressing wild-type TRPV5 displayed $Ca^{2+}$ and $Na^{+}$ currents in line with our previous studies, including a high $Ca^{2+}$ selectivity over $Na^{+}$, the presence of large $Na^{+}$ currents in the absence of extracellular divalent ions and strong inward rectification (Vennekens *et al*., 2000). The T600A mutant of TRPV5 failed to produce significant $Na^{+}$ and $Ca^{2+}$ currents in HEK293 cells in the absence and presence of extracellular $Ca^{2+}$, respectively, while the channel was readily detectable by immunoblotting. Likewise, the corresponding mutant in TRPV6 (T599A) expressed in HEK293 cells was functionally inactive. Notably, HEK293 cells endogenously expressed S100A10 and annexin 2 as confirmed by RT–PCR analysis (data not shown). Thus, these findings suggested that the binding of S100A10 to TRPV5 and TRPV6 is crucial to obtain channel activity.

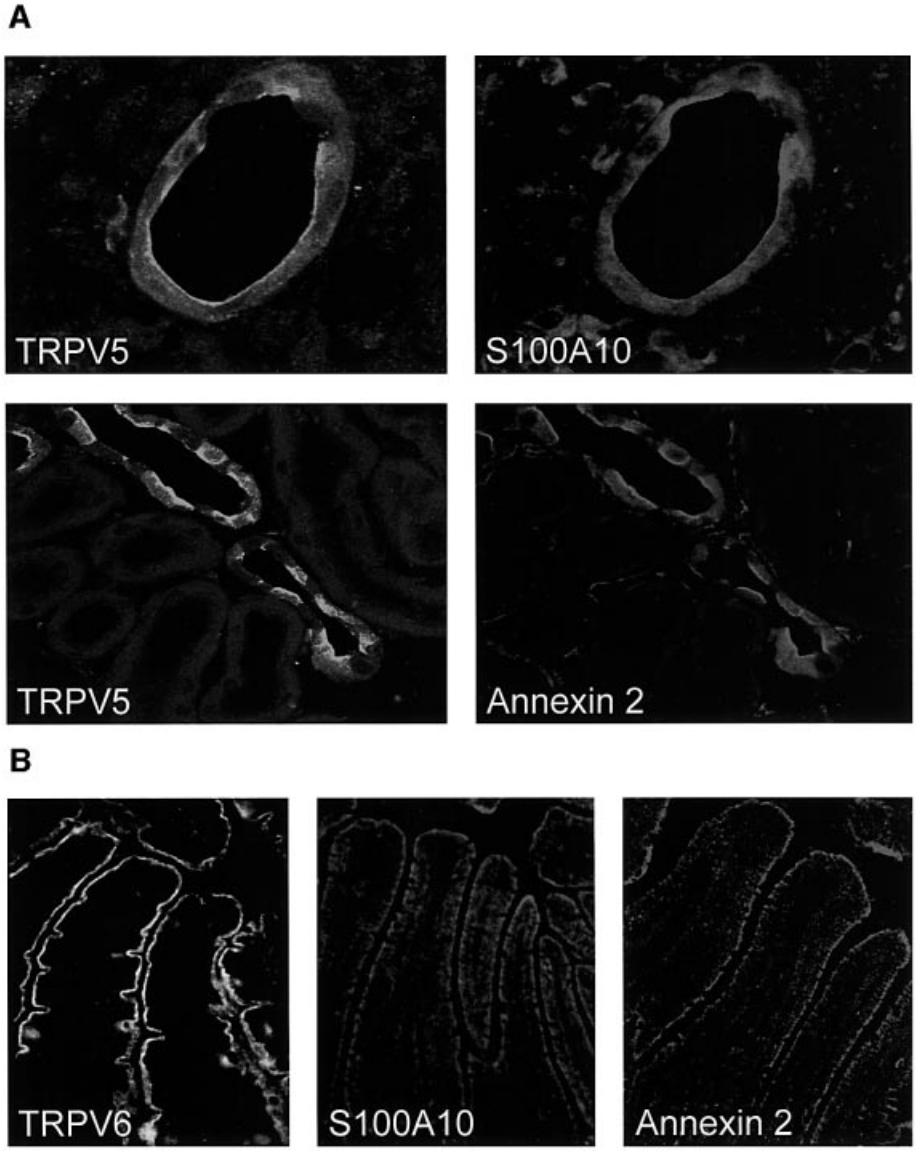


**Fig. 3.** Colocalization of TRPV5 and TRPV6 with S100A10 and annexin 2. (**A**) Kidney sections were costained with antibodies against TRPV5 and S100A10 or TRPV5 and annexin 2. (**B**) Duodenum sections were stained with antibodies against TRPV6, S100A10 and annexin 2. See Supplementary data for color images of this figure.

### *S100A10 is essential for trafficking of TRPV5 and TRPV6*

The role of S100A10 in the routing of TRPV5 and TRPV6 was investigated using *X.laevis* oocytes, as shown in Figure 5C. Immunocytochemical analysis of TRPV5 or TRPV6 cRNA-injected oocytes demonstrated a strong immunopositive labeling of the plasma membrane for both channels, whereas the cytoplasm was only faintly stained. This finding suggests that wild-type TRPV5 and TRPV6 are targeted efficiently to the plasma membrane. In contrast, the subcellular localization of the TRPV5 T600A and TRPV6 T599A mutants was seriously disturbed. The plasma membrane was virtually devoid of immunopositive staining for these mutant channels, but instead a strong immunopositive signal accumulated in an area just below the plasma membrane. Notably, *X.laevis* oocytes endogenously express S100A10 and annexin 2 as demonstrated by RT–PCR analysis. Taken together, these results imply that the association of S100A10 is necessary for correct trafficking (i.e. targeting or retention) of TRPV5 and TRPV6 to the plasma membrane.

### *Gene silencing of annexin 2 using RNAi*

The use of small interfering RNAs (siRNAs) has become a powerful tool to knock down specific gene expression in mammalian cell lines including HEK293 cells (Caplen *et al*., 2001; Elbashir *et al*., 2001). We have, therefore, applied this novel technique to further substantiate the role of annexin 2 in the regulation of $Ca^{2+}$-channel activity. First, HEK293 cells were transfected with annexin 2-specific siRNAs, subsequently with the pIRES-TRPV5 or pIRES-TRPV6 vector and finally analyzed by immunoblotting, immunofluorescence and patch–clamp as shown in Figure 6. Annexin 2 expression was significantly downregulated by annexin 2-specific siRNA transfection (Figure 6A), while the expression of TRPV5 and TRPV6

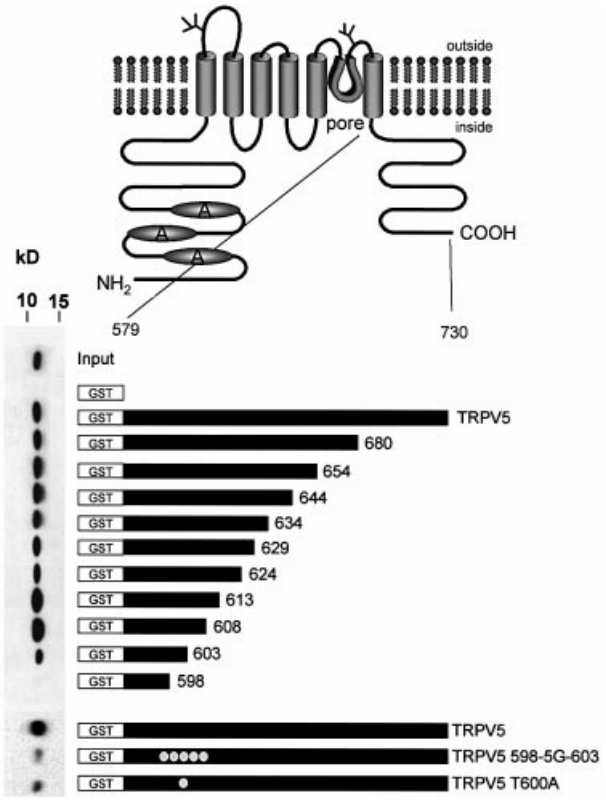


**Fig. 4.** Mapping of the S100A10 binding site in TRPV5. GST fusion proteins containing different portions of the C-terminal tail of TRPV5 were constructed according to the schematic drawing. These proteins were immobilized on glutathione–Sepharose 4B beads and then incubated with lysates from *X.laevis* oocytes injected with 20 ng of S100A10 cRNA. Interaction of S100A10 with the GST fusion proteins was determined by immunoblotting. The binding site was localized between amino acids 598 and 603. Virtually all interaction with S100A10 was abolished when this region (VATTV) was mutated into glycines. A similar effect was observed with the single point mutant TRPV5 T600A.

was not affected in these cells (Figure 6C), demonstrating the specificity of the RNAi. In addition, we observed a decrease in S100A10 expression (Figure 6B), most likely due to a decreased stability of the S100A10 protein in the absence of annexin 2 (Puisieux *et al*., 1996). In line with these immunoblot results, the number of annexin 2-immunopositive cells significantly decreased following siRNA transfection as determined by fluorescence microscopy (Figure 6D and E). In these experiments the $Na^+$ currents were determined by patch–clamp analysis as a direct measure of channel activity. Control HEK293 cells heterologously expressing TRPV5 exhibited a normal distribution of the $Na^+$ current with a peak around 800 pA/pF (Figure 6H). Interestingly, HEK293 cells cotransfected with annexin 2-specific siRNAs and TRPV5 demonstrated a shift in the distribution of the $Na^+$ current, possibly resulting from two different populations of cells (Figure 6H). A minority of cells exhibited a normal $Na^+$ current reflecting annexin 2-expressing cells, while in the majority of cells only a small current was measured (Figure 6F and G), reflecting annexin 2 downregulated cells. Identical results were obtained for TRPV6 in the annexin 2 siRNA-treated cells. Also, when the current was averaged over the total population of cells a significant decrease in the $Na^+$ current was apparent for both TRPV5 and TRPV6 (Figure 6I).

### *Hormonal regulation of S100A10*

Recently, we have shown that the TRPV5 and TRPV6 expression levels in kidney and duodenum are positively regulated by 1,25-dihydroxyvitamin $D_3$ [$1,25(OH)_2D_3$] in vitamin D receptor and 1α-OHase knockout mice, animal models for pseudovitamin D-deficiency rickets (Van Cromphaut *et al*., 2001; Hoenderop *et al*., 2002a). The renal expression level of S100A10 was, therefore, analyzed under identical circumstances. Treatment with $1,25(OH)_2D_3$ significantly upregulated the mRNA abundance of S100A10 (158 ± 16% compared with control levels, $P < 0.05$). Thus, in kidney, S100A10 is, like TRPV5, upregulated by $1,25(OH)_2D_3$.

## Discussion

The present study identified the S100A10–annexin 2 pair as the first auxiliary protein complex for the newly identified epithelial $Ca^{2+}$ channels, TRPV5 and TRPV6. S100A10 forms a well-defined heteromeric complex with annexin 2 and associates specifically with the conserved sequence VATTV located in the C-terminal tail of TRPV5 and TRPV6. Of these five amino acids, the first threonine residue plays a crucial role since the corresponding channel mutants preclude S100A10 binding and accumulate below the plasma membrane preventing the facilitation of $Ca^{2+}$ inward currents.

### *S100A10–annexin 2 complex associates with TRPV5 and TRPV6*

S100A10 was initially identified as a TRPV5-interacting protein by a yeast two-hybrid screening, and the binding between both proteins was subsequently confirmed by GST pull-down assays. The binding was not restricted to TRPV5 since TRPV6 was also shown to bind S100A10, indicating a mutual mechanism in the regulation of these $Ca^{2+}$ channels. Considering the high degree of homology and the similarities in electrophysiological behavior between both channels (Hoenderop *et al*., 2001b), it is indeed likely that TRPV5 and TRPV6 have common regulatory factors such as associated regulatory proteins. S100A10 is a distinct member of the S100 family, since its two EF hands carry mutations that render it $Ca^{2+}$ insensitive (Gerke and Weber, 1985), explaining the $Ca^{2+}$-independent association with TRPV5. Furthermore, we could show by co-immunoprecipitations and GST pull-down experiments that the membrane-associated and microfilament-binding protein, annexin 2, is part of the channel–S100A10 complex. Employing lysates from cells co-expressing TRPV5 and S100A10/annexin 2, we were not able to immunoprecipitate S100A10 and annexin 2 together with TRPV5 using anti-TRPV5 antibodies (data not shown). The physical association of the S100A10–annexin 2 complex with TRPV5 could be too weak to resist detergent solubilization, or could be spatially restricted to the plasma membrane, only locally regulating TRPV5 and TRPV6. Both scenarios would preclude an efficient co-immunoprecipitation. Interestingly, an association of annexin 2 with TRPV5 could be shown only in the

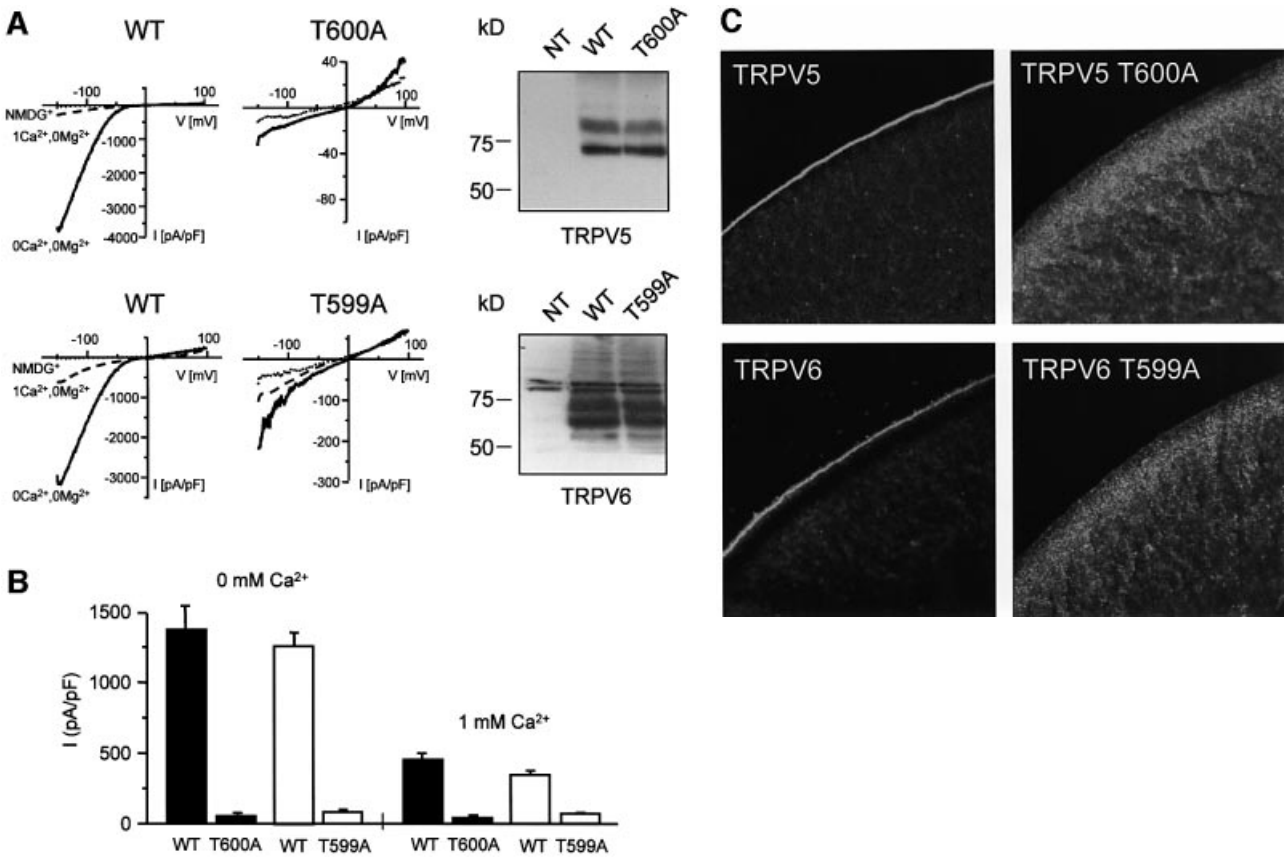


**Fig. 5.** Activity and subcellular localization of TRPV5 and TRPV6 with a mutated S100A10 binding site. HEK293 cells were transiently transfected with TRPV5 (wild type or T600A) or TRPV6 (wild type or T599A) and analyzed using the whole-cell patch–clamp configuration and immunoblotting. (**A**) Currents were measured during voltage ramps from –150 to +100 mV (400 ms) in the absence of permeable cations (all substituted by $NMDG^+$), in the absence of divalent cations only, and in the presence of 1 mM $Ca^{2+}$. The *I/V* curves showed inward rectification typical for TRPV5 and TRPV6. In the TRPV5 T600A and TRPV6 T599A mutants $Na^+$ and $Ca^{2+}$ currents were virtually abolished, while the channel was readily detectable. NT, not transfected. (**B**) The average currents measured in the absence of divalent cations and in the presence of 1 mM $Ca^{2+}$ of three independent transfections for wild-type and mutant TRPV5 and TRPV6 are depicted. (**C**) Immunocytochemistry was performed on *X.laevis* oocytes injected with 5 ng of HA-tagged TRPV5 (wild type or T600A) or Flag-tagged TRPV6 (wild type or T599A) cRNA. Oocytes injected with wild-type channels showed predominant immunopositive staining at the plasma membrane, whereas the channels containing a mutation in the S100A10 binding site accumulated in an area just below the plasma membrane. Representative images of three independent experiments are shown.

presence of S100A10, demonstrating that annexin binds indirectly to the TRPV5 C-terminal tail, with S100A10 most likely operating as a bridge between TRPV5 and annexin 2. Annexin 2 forms a heterotetrameric complex with S100A10, consisting of a S100A10 dimer associated with the N-terminal tails of two annexin 2 molecules in a highly symmetric manner (Rety *et al*., 1999). Furthermore, we have recently demonstrated that TRPV5 and TRPV6 form homo- and heterotetramic channel complexes, which possibly create four S100A10 binding sites per functional channel (Hoenderop *et al*., 2003). Taken together, TRPV5 and TRPV6 interact with the S100A10–annexin 2 heteromultimer possibly with four available interaction sites.

### *Co-localization of S100A10–annexin 2 complex and the epithelial $Ca^{2+}$ channels in kidney and duodenum*

In kidney, TRPV5 is primarily expressed along the apical membrane of distal convoluted and connecting tubules (Hoenderop *et al*., 2000; Loffing *et al*., 2001). Importantly, S100A10 and annexin 2 were consistently detected in these TRPV5-expressing tubules, where they concentrated along the apical membrane. Furthermore, the S100A10–annexin 2 complex was present along the brush-border membrane of duodenum, which is in agreement with the TRPV6 localization. S100A10 and annexin 2 were previously identified in placenta and pancreas, sites with a prominent TRPV5 and TRPV6 expression (Kaczan-Bourgois *et al*., 1996; Dreier *et al*., 1998; Massey-Harroche *et al*., 1998; Hoenderop *et al*., 1999a; Wissenbach *et al*., 2001; Janssen *et al*., 2002). Generally, the S100A10–annexin 2 complex is localized to the cytoskeleton underlying the plasma membrane (Thiel *et al*., 1992; Zobiack *et al*., 2001) and it has been proposed to participate in membrane trafficking and/or organization in this area of the cell (Gerke and Moss, 2002). Thus, the observed apical localization of the S100A10–annexin 2 complex in TRPV5- and TRPV6-expressing epithelia is in line with a regulatory role in the plasma membrane localization of the $Ca^{2+}$ channels and thus their function in the process of $Ca^{2+}$ (re)absorption.

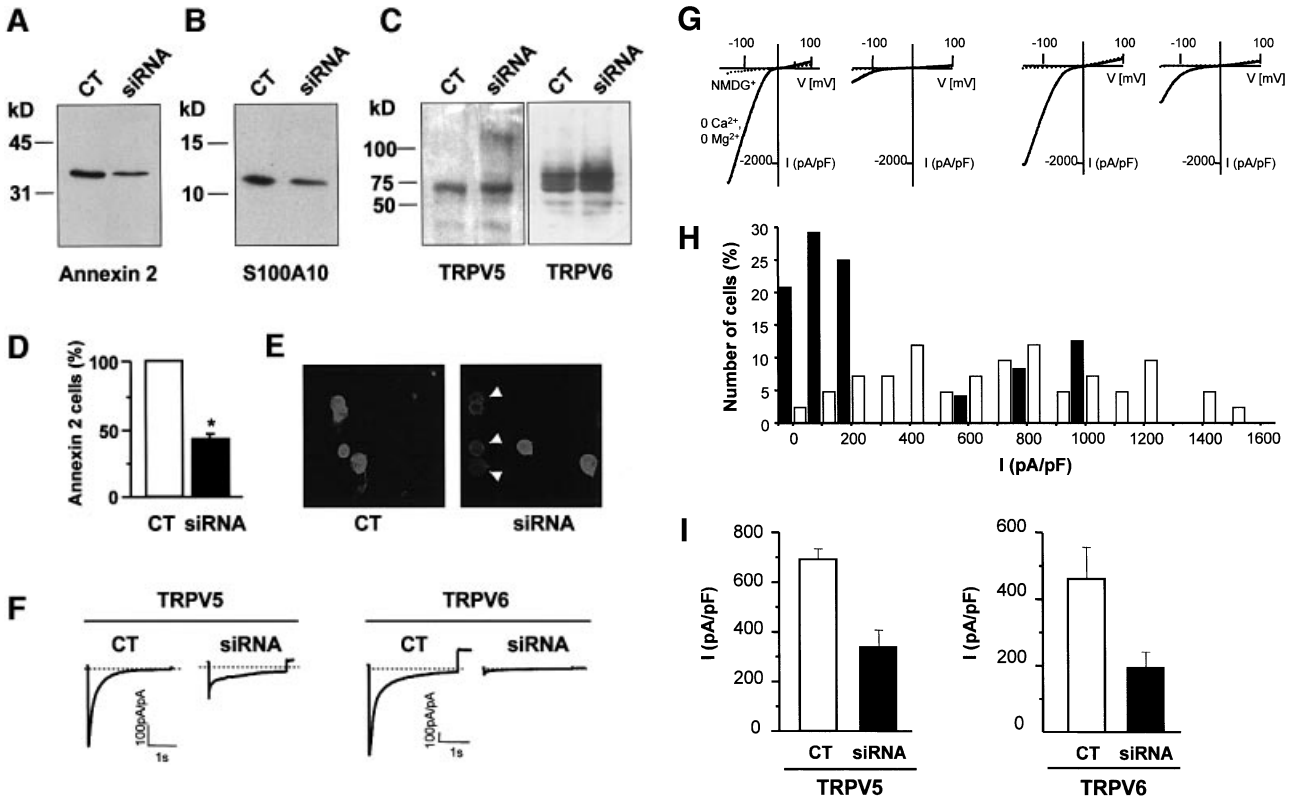


**Fig. 6.** SiRNA-mediated annexin 2 gene silencing inhibits channel activity in HEK293 cells heterologously expressing TRPV5. Immunoblot showing annexin 2 (**A**), S100A10 (**B**), TRPV5 and TRPV6 (**C**) protein levels in control (CT) and annexin 2-specific siRNA-treated HEK293 cells. Images (**E**) and corresponding histogram (**D**) of annexin 2 immunofluorescence staining of control and annexin 2-specific siRNA transfected HEK293 cells. $Ca^{2+}$ currents in response to a voltage step from +20 to –100 mV in control and annexin 2-specific siRNA transfected HEK293 cells (**F**). Current response to a voltage ramp from –150 to 100 mV measured in $NMDG^+$ and divalent-free solution in control and annexin 2-specific siRNA transfected HEK293 cells (**G**). Distribution of $Na^+$ currents as a measure of channel activity analyzed in control (open bars) and annexin 2-specific siRNA-transfected (closed bars) HEK293 cells at –80 mV (**H**) and the corresponding averaged data (**I**). *N* is more than 25 cells of two independent transfections. $^*P < 0.001$ significantly different from control. CT, control.

### *S100A10 interaction with TRPV5 and TRPV6 is essential for trafficking*

The association of S100A10 with TRPV5 and TRPV6 was restricted to a short peptide sequence VATTV located in the C-terminal tail of these channels. This stretch is completely conserved among all identified species of TRPV5 and TRPV6 (Hoenderop *et al.*, 2001b). Interestingly, the TTV sequence in the S100A10 binding motif resembles an internal type I PDZ consensus binding sequence, which is S/TXV (Songyang *et al.*, 1997). However, S100A10 does not contain PDZ domains, indicating that the TRPV5–S100A10 interaction has a different nature. The first threonine of the S100A10 interaction motif was identified as a crucial determinant for binding. Furthermore, the activity of TRPV5 and TRPV6 was abolished when this particular threonine was mutated, demonstrating that this motif is essential for channel function. Malfunctioning of these mutant channels was accompanied by a major disturbance in their subcellular localization. These findings suggest a role for the S100A10–annexin 2 heterotetramer in the trafficking process of TRPV5 and TRPV6 to the plasma membrane. Whether this involves facilitated translocation of TRPV5 and TRPV6 channels to the plasma membrane or enhancement of channel retention remains to be elucidated.

Recently, S100A10 was demonstrated to interact with the background $K^+$ channel TASK-1, controlling the membrane trafficking and, therefore, the functionality of this $K^+$ channel (Girard *et al.*, 2002). TASK-1 associated with S100A10 via its C-terminal sequence SSV. This sequence resembles the binding motif in TRPV5 and TRPV6 identified in the present study, suggesting a shared structural S100A10 binding pocket. However, this motif is absent in the tetrodotoxin-insensitive voltage-gated $Na^+$ channel ($Na_v1.8$), which has been shown to bind S100A10 via its N-terminal tail (Okuse *et al.*, 2002). This S100A10 interaction promoted the translocating of $Na_v1.8$ to the plasma membrane producing functional $Na^+$ channels.

### *Role of annexin 2 in $Ca^{2+}$-channel activity*

S100A10 is predominantly present as a heterotetrameric complex with annexin 2, which has been implicated in numerous biological processes including endocytosis, exocytosis and membrane–cytoskeleton interactions (Ali *et al.*, 1989; Gerke and Moss, 2002). Annexin 2 is postulated to bind to the cytoplasmic face of membrane rafts to stabilize these domains, thereby providing a link to the actin cytoskeleton. The present study demonstrated the presence of annexin 2 in the S100A10–channel complex, indicating a possible function in regulating

channel localization and/or activity. Importantly, down-regulation of annexin 2 using annexin 2-specific siRNAs significantly inhibited the currents through TRPV5, indicating that annexin 2 in conjunction with S100A10 is crucial for TRPV5 activity. In line with the cortical localization of annexin 2 and its postulated function in organizing certain plasma membrane domains, our findings provided the first functional evidence for a regulatory role of annexin 2 controlling $Ca^{2+}$ channel trafficking. A role of annexin 2 was neither assessed for TASK-1 nor $Na_v1.8$ (Girard *et al*., 2002; Okuse *et al*., 2002). It remains, therefore, to be determined whether annexin 2 also mediates the regulatory role of S100A10 for these ion channels. Importantly, annexin 2 has been shown to modulate the activity of volume-activated $Cl^-$ channels in vascular endothelial cells (Nilius *et al*., 1996). Disruption of the S100A10–annexin 2 complex resulted in a gradual decrease of $Cl^-$ current, possibly indicating a decrease of functional channels at the plasma membrane. These findings, together with our data, clearly show that the S100A10–annexin 2 complex is a significant component for the trafficking of different ion channels to the plasma membrane and is thus a major regulator of ion homeostasis.

### *Regulation of S100A10*

Vitamin D is an important calciotropic hormone determining the $Ca^{2+}$ balance in the body. An increase in functional expression of TRPV5 and TRPV6 has been implicated as one of the major determinants of long-term vitamin D efficacy (Hoenderop *et al*., 2001a, 2002a; Van Cromphaut *et al*., 2001). Here, we indicated that S100A10 abundance, analogous to TRPV5 and TRPV6, is regulated by $1,25(OH_2)D_3$. In addition, annexin 2 expression levels have been shown to increase upon prolonged incubation with $1,25(OH_2)D_3$ (Menaa *et al*., 1999). Together, our observations imply that $1,25(OH_2)D_3$ exerts a major calciotropic effect by concomitantly increasing the S100A10, annexin 2 and epithelial $Ca^{2+}$-channel expression and thus efficiently stimulating $Ca^{2+}$-channel recruitment during $Ca^{2+}$ demand.

In conclusion, our data provided the first evidence of a regulatory role for the S100A10–annexin 2 heterotetramer in vitamin D-mediated $Ca^{2+}$ (re)absorption in general and in particular in TRPV5 and TRPV6 routing. The elucidated molecular mechanism involves tethering of the S100A10–annexin 2 complex to the $Ca^{2+}$ channel, resulting in functional plasma membrane localization. This mechanism is likely applicable to other ion transporters given the wide tissue distribution of S100A10 and the associated annexin 2 protein.

## Materials and methods

### *DNA constructs and cRNA synthesis*

The C-terminal tail of mouse TRPV5 was amplified using PCR (forward primer 5′-CCCCTGGGATCCGGCGACACTCACTGGCGAGTGGCC-3′ and reverse primer 5′-ACAGAAGTCGACTCAGAAATGGTA-GATCTCCTC-3′) on mouse kidney cDNA and cloned in the pAS-1 yeast cloning and expression vector, which was kindly provided by Dr Steve Elledge (Baylor College of Medicine, Houston, TX). The product was sequenced and compared with three independent mouse cDNAs to confirm the sequence. The C-terminal tail of mouse TRPV5 and TRPV6 was subcloned into pGEX6p-2 (Amersham Pharmacia Biotech). Deletion mutants of TRPV5 were obtained by PCR and cloned into pGEX6p-2. Full-length mouse S100A10 cDNA was subcloned into pGEX6p-2 by PCR (forward primer 5′-CGCGGGATCCATGCCATCCCAAATGGAG-CAC-3′ and reverse primer 5′-GCTCCAGATATCCTACTTCTTCCCC-TTCTGCTT-3′) using the S100A10 pACT2 construct as a template. Annexin 2 was obtained using PCR (forward primer 5′-GCTCTA-GATGTCTACTGTCCACGAAATCC-3′ and reverse primer 5′-CGAA-GTCTCTAGAACGCCAGG-3′) on mouse kidney cDNA and cloned into pT7Ts (Krieg and Melton, 1984). A VSV epitope tag was fused to the N-terminal tail of S100A10 by PCR (forward primer 5′-GAAGA-TCTATGGAGATTTATACAGACATAGAGATGAACCGACTTGGA-AAGCTTATGCCATCCCAAATGGAG-3′ and reverse primer 5′-GC-TCCAGATATCCTACTTCTTCCCCTTCTGCTT-3′) using the pACT2 construct as a template, and the obtained product was subcloned into pT7Ts. Wild-type TRPV5 and TRPV6 were tagged at the N-terminal tail with a HA and Flag tag, respectively. The N-terminally tagged fragments were amplified by PCR using, for TRPV5, forward primer 5′-CAGATCGCGAGCCACCATGTACCCATACGACGTGCCAGACTA-CGCAGGGGCCTGTCCACCCAAGGCA-3′ and reverse primer 5′-CCCAGGGAGTCCTGGGCCCGG-3′, and for TRPV6, forward primer 5′-CAGATCGCGAGCCACCATGGACTACAAGGATGACGATGAC-AAGGGGTGGTCCCTGCCCAAGGAGAAG-3′ and reverse primer 5′-GGACAAAGGGTGCTCTCCATA-3′, with the wild-type TRPV5 and TRPV6 pTLN constructs as templates. The obtained fragments were subsequently cloned into the pTLN vector (Steinmeyer *et al*., 1995). Oocyte expression constructs were linearized and TRPV5, TRPV6, annexin 2 and S100A10 cRNA were synthesized *in vitro* using SP6 RNA polymerase for TRPV5 and TRPV6, and T7 RNA polymerase for annexin 2 and S100A10 as described previously (Hoenderop *et al*., 1999b). All constructs were verified by sequence analysis.

### *Yeast two-hybrid system*

The Y153 yeast strain (Durfee *et al*., 1993) was first transformed to Trp prototrophy with pAS-1 containing the TRPV5 C-terminal tail. Expression of the Gal4-TRPV5 hybrid protein was confirmed by immunoblotting using monoclonal antibodies against the HA epitope (Sigma). Yeast was transformed with a mouse kidney cDNA library (Clontech) present in the pACT2 vector, containing a leucine selection marker. Subsequently, yeast cells were plated onto Trp–Leu–His selective medium supplemented with 25 mM 3-aminotriazole. Positive colonies were assayed for β-galactosidase activity as described previously (Vojtek *et al*., 1993). Yeast DNA of positive colonies was isolated (Hoffman and Winston, 1987), and prey plasmids were rescued by transformation into KC8 cells, which carry *trpC*, *leuB* and *hisB* mutations (Clontech). Yeast two-hybrid results were confirmed using purified library plasmids and negative controls were performed by replacing a binding partner with either a pAS-1 construct containing the N-terminal tail (amino acids 1–53) of rat γENaC (Firsov *et al*., 1999) or the empty pACT2 vector.

### *GST–TRPV5 fusion protein and interaction assays*

pGEX6p-2 constructs were transformed in *Escherichia coli* BL21, and GST fusion proteins were expressed and purified according to the manufacturer's protocol (Amersham Pharmacia Biotech). *Xenopus laevis* oocytes were injected with 20 ng of S100A10 cRNA, 20 ng of annexin 2 cRNA, or co-injected with 10 ng of S100A10 cRNA and 10 ng of annexin 2 cRNA as described elsewhere (Hoenderop *et al*., 1999a). After 48–72 h, oocytes were homogenized in pull-down buffer [20 mM Tris–HCl pH 7.4, 140 mM NaCl, 1 mM $CaCl_2$, 0.2% (v/v) Triton X-100 and 0.2% (v/v) NP-40] and centrifuged twice for 10 min at 16 000 *g*. Oocyte supernatants were added to GST or GST–TRPV5 fusion proteins immobilized on glutathione–Sepharose 4B beads (Amersham Pharmacia Biotech). [$^{35}$S]methionine-labeled full-length TRPV5 protein was prepared using a reticulocyte lysate system in the presence of canine microsomal membranes (Promega) and added to GST or GST–S100A10 immobilized on glutathione–Sepharose 4B beads. After 2 h incubation at room temperature, the beads were washed extensively with pull-down buffer. Bound proteins were eluted with SDS–PAGE loading buffer, separated on SDS–PAGE gels and visualized either by autoradiography (for TRPV5 and TRPV6) or immunoblotting using monoclonal anti-VSV (1:10 000 clone P5D4; Sigma) (for S100A10) or monoclonal anti-annexin 2 (1:5000; Transduction Laboratories).

### *Co-immunoprecipitation*

For chemical cross-linking experiments, 20 ng of S100A10 cRNA injected oocytes were lysed in 20 mM HEPES pH 7.2, 5 mM KCl, 130 mM NaCl, 5 mM EDTA and 10% (v/v) glycerol containing 2 mM

DTBP (Pierce) incubated on ice for 30 min, and 100 mM Tris–HCl pH 7.4 was added. The lysates were centrifuged for 30 min at 16 000 *g* and supernatant was analyzed by immunoblot as described above. For co-immunoprecipitation experiments, S100A10 and annexin 2 cRNA co-injected oocytes were labeled with [$^{35}$S]methionine for 48 h and homogenized in pull-down buffer containing 2 mM EDTA instead of 1 mM $CaCl_2$ to allow for annexin 2 solubilization. Oocyte homogenates were centrifuged twice for 10 min at 16 000 *g*. Supernatants were incubated with anti-VSV antibodies immobilized on protein A–agarose beads (Kem-En-Tec A/S, Copenhagen, Denmark) for 2 h at room temperature. After three washing steps with pull-down buffer, immunoprecipitated proteins were eluted with SDS–PAGE loading buffer, separated on SDS–PAGE gel and visualized by autoradiography.

### *RT–PCR analysis*

Total RNA from mouse kidney, mouse duodenum, HEK293 and *X.laevis* oocytes was isolated using Trizol (Gibco BRL). Total RNA (2 µg) was reverse transcribed and PCR reactions for S100A10 and annexin 2 were performed (S100A10 forward primer 5′-GCCATGGAAACCATGATG-3′ and reverse primer 5′-AAATAGTCATTGCATGCAATG-3′; annexin 2 forward primer 5′-ATGTCTACTGTTCACGAAATC-3′ and reverse primer 5′-CCCCTTCATGGAAGCTTTTAG-3′). For PCR analysis of oocyte mRNA different primers were used (S100A10 forward 5′-GATGGTGGCCCCCTCTGA-3′ and reverse primer 5′-CCACAAGTT-TAGAGTTTA-3′; annexin 2 forward primer 5′-GCTGCACCTACA-GCTGCT-3′ and reverse primer 5′-CTTTATTTGTCCTGGAGC-3′).

### *Real-time quantitative PCR*

1α-OHase knockout mice were supplemented with $1,25(OH)_2D_3$ as described previously (Hoenderop *et al*., 2002a). S100A10 mRNA expression levels in kidney were quantified by real-time quantitative PCR using the ABI Prism 7700 Sequence Detection System (PE Biosystems, Rotkreuz, Switzerland) as described previously (Hoenderop *et al*., 2002a) (forward primer 5′-TGCCATCCCAAATGGAGC-3′, reverse primer 5′-TCGCCTGCAAACCTGTGAA-3′ and probe 5′-CGC-CATGGAAACCATGATGCTTACG-3′). The expression level of mouse hypoxanthine–guanine phosphoribosyl transferase (HPRT) was detected with the forward primer 5′-TTATCAGACTGAAGAGCTACTGTAAT-GATC-3′, reverse primer 5′-TTACCAGTGTCAATTATATCTTCAA-CAATC-3′ and probe 5′-TGAGAGATCATCTCCACCAATAACT-TTTATGTCCC-3′, and used as an endogenous control to normalize variations in RNA extractions, the degree of RNA degradation and variabilities in RT efficiencies.

### *Immunohistochemistry*

Immunohistochemistry was performed as described previously (Hoenderop *et al*., 2001a). Briefly, rat and rabbit duodenum sections were incubated for 16 h at 4°C with rabbit antiserum against TRPV6 (1:100) kindly provided by Dr M.Suzuki (Jichi Medical School, Tochigi, Japan), monoclonal anti-S100A10 (1:50; Swant, Bellinzona, Switzerland) or monoclonal anti-annexin 2 (1:50; Transduction Laboratories). Rabbit kidney sections were incubated for 16 h at 4°C with affinity purified guinea pig antiserum against TRPV5 (1:50; Hoenderop *et al*., 2000) and monoclonal anti-S100A10 (1:100) or monoclonal anti-annexin 2 (1:50). To visualize TRPV5 and TRPV6, a goat anti-guinea pig Alexa 488 conjugated antibody (1:300) or a goat anti-rabbit Alexa 488 conjugated antibody (1:300; Molecular Probes) was used. To visualize S100A10 and annexin 2, sections were incubated with a goat anti-mouse Alexa 594 conjugated antibody (1:300; Molecular Probes). *Xenopus laevis* oocytes were injected with 5 ng of HA-tagged TRPV5 (wild type or T600A) or Flag-tagged TRPV6 (wild type or T599A) cRNA. Three days after injection immunocytochemistry was performed as described previously (Hoenderop *et al*., 1999b) using monoclonal anti-HA (1:400; Sigma) or monoclonal anti-Flag (1:400; Sigma). Images were taken with a Bio-Rad MRC 100 confocal laser scanning microscope. All negative controls, including sections incubated with pre-immune serum or conjugated antibodies alone, were devoid of any staining.

### *Electrophysiology*

The full-length cDNA encoding TRPV5 and TRPV6 was cloned into the pIRES vector and transfected in HEK293 as described previously (Vennekens *et al*., 2000; Hoenderop *et al*., 2001b). Currents using the whole-cell configuration were measured with an EPC-9 (HEKA Elektronik, Lambrecht, Germany; 8-Pole Bessel filter 10 kHz). Electrode resistances were between 2 and 5 MΩ, capacitance and series resistance were compensated, and access resistance was monitored continuously. Current–voltage (*I*/*V*) relationships were measured from linear 400 ms voltage ramps, which were applied every 5 s from a holding potential of +20 or +70 mV with a sampling interval of 0.8 ms. The step protocol consisted of 3 s voltage steps to –100 mV from a holding potential of +70 mV. The standard extracellular solution contained 150 mM NaCl, 1 mM $CaCl_2$, 6 mM CsCl, 1 mM $MgCl_2$, 10 mM glucose and 10 mM HEPES/CsOH pH 7.4. Monovalent cation currents were measured in nominally $Ca^{2+}$- and $Mg^{2+}$-free solution (free $Ca^{2+}$ concentration is 10 nM), and $Ca^{2+}$ currents in 1 mM $CaCl_2$ but $Mg^{2+}$-free solutions. Monovalent cation currents were inhibited by replacing 150 mM NaCl with an equimolar amount of *N*-methyl-D-glucamine (NMDG)-Cl. The standard internal (pipette) solution contained: 20 mM CsCl, 100 mM Cs aspartate, 1 mM $MgCl_2$, 10 mM BAPTA, 4 mM $Na_2ATP$ and 10 mM HEPES/CsOH pH 7.2. Cells were kept in a nominally $Ca^{2+}$-free medium to prevent $Ca^{2+}$ overload, and exposed for a maximum of 5 min to a Krebs solution containing 1.5 mM $Ca^{2+}$ before sealing the patch pipette to the cell. In the siRNA experiments, 0.5 mM EGTA was used for intracellular $Ca^{2+}$ buffering. All experiments were performed at room temperature (20–22°C).

### *RNAi*

RNAi employed a 21 nucleotide RNA duplex corresponding in sequence to nucleotides 94–113 of the human annexin 2 mRNA with a two nucleotide dT 3′ overhang. Cells grown on coverslips were transfected with 100 nM of the annealed RNA duplex using oligofectamine according to the manufacturer's instructions (Invitrogen). After 24 h these siRNA transfected HEK293 cells were transfected with pIRES-TRPV5 or pIRES-TRPV6 vector and analyzed in a patch–clamp setup 24 h following the last transfection. Expression of TRPV5 and TRPV6 was determined using immunoblotting with affinity-purified guinea pig (TRPV5) or rabbit (TRPV6) antibodies as described elsewhere (Hoenderop *et al*., 2003).

### *Statistical analysis*

In all experiments, the data are expressed as mean ± SEM. Overall statistical significance was determined by analysis of variance (ANOVA). In the case of significance ($P < 0.05$), individual groups were compared by Student's *t*-test.

### *Supplementary data*

Supplementary data are available at *The EMBO Journal* Online.

## Acknowledgements

The authors thank Susan Hoefs and Annemiete van der Kemp for excellent technical support. This work was supported by the Dutch Organization of Scientific Research (Zon-Mw 016.006.001, Zon-Mw 902.18.298, NWO-ALW 810.38.004, NWO-ALW 805.09.042) and in part by the Belgian Federal Government, the Flemish Government and the Onderzoeksraad KU Leuven (GOA 99/07, F.W.O. G.0237.95, F.W.O. G.0214.99, F.W.O. G.0136.00, F.W.O. 0172.03), a grant from the 'Alphonse and Jean Forton–Koning Boudewijn Stichting' R7115 B0 and the Deutsche Forschungsgemeinschaft (Ge 514/4-3).

## References

Ali,S.M., Geisow,M.J. and Burgoyne,R.D. (1989) A role for calpactin in calcium-dependent exocytosis in adrenal chromaffin cells. *Nature*, **340**, 313–315.

Caplen,N.J., Parrish,S., Imani,F., Fire,A. and Morgan,R.A. (2001) Specific inhibition of gene expression by small double-stranded RNAs in invertebrate and vertebrate systems. *Proc. Natl Acad. Sci. USA*, **98**, 9742–9747.

Dreier,R., Schmid,K.W., Gerke,V. and Riehemann,K. (1998) Differential expression of annexins I, II and IV in human tissues: an immunohistochemical study. *Histochem. Cell Biol.*, **110**, 137–148.

Durfee,T., Becherer,K., Chen,P.L., Yeh,S.H., Yang,Y., Kilburn,A.E., Lee,W.H. and Elledge,S.J. (1993) The retinoblastoma protein associates with the protein phosphatase type 1 catalytic subunit. *Genes Dev.*, **7**, 555–569.

Elbashir,S.M., Harborth,J., Lendeckel,W., Yalcin,A., Weber,K. and Tuschl,T. (2001) Duplexes of 21-nucleotide RNAs mediate RNA interference in cultured mammalian cells. *Nature*, **411**, 494–498.

Firsov,D., Robert-Nicoud,M., Gruender,S., Schild,L. and Rossier,B.C. (1999) Mutational analysis of cysteine-rich domains of the epithelium

sodium channel (ENaC). Identification of cysteines essential for channel expression at the cell surface. *J. Biol. Chem.*, **274**, 2743–2749.
Gerke,V. and Moss,S.E. (2002) Annexins: from structure to function. *Physiol. Rev.*, **82**, 331–371.
Gerke,V. and Weber,K. (1985) The regulatory chain in the p36-kd substrate complex of viral tyrosine-specific protein kinases is related in sequence to the S-100 protein of glial cells. *EMBO J.*, **4**, 2917–2920.
Girard,C., Tinel,N., Terrenoire,C., Romey,G., Lazdunski,M. and Borsotto,M. (2002) p11, an annexin II subunit, an auxiliary protein associated with the background $K^+$ channel, TASK-1. *EMBO J.*, **21**, 4439–4448.
Hoenderop,J.G., van der Kemp,A.W., Hartog,A., van de Graaf,S.F., van Os,C.H., Willems,P.H. and Bindels,R.J. (1999a) Molecular identification of the apical $Ca^{2+}$ channel in 1,25-dihydroxyvitamin $D_3$-responsive epithelia. *J. Biol. Chem.*, **274**, 8375–8378.
Hoenderop,J.G., van der Kemp,A.W., Hartog,A., van Os,C.H., Willems,P.H. and Bindels,R.J. (1999b) The epithelial calcium channel, ECaC, is activated by hyperpolarization and regulated by cytosolic calcium. *Biochem. Biophys. Res. Commun.*, **261**, 488–492.
Hoenderop,J.G., Hartog,A., Stuiver,M., Doucet,A., Willems,P.H. and Bindels,R.J. (2000) Localization of the epithelial $Ca^{2+}$ channel in rabbit kidney and intestine. *J. Am. Soc. Nephrol.*, **11**, 1171–1178.
Hoenderop,J.G. *et al.* (2001a) Calcitriol controls the epithelial calcium channel in kidney. *J. Am. Soc. Nephrol.*, **12**, 1342–1349.
Hoenderop,J.G., Vennekens,R., Muller,D., Prenen,J., Droogmans,G., Bindels,R.J. and Nilius,B. (2001b) Function and expression of the epithelial $Ca^{2+}$ channel family: comparison of mammalian ECaC1 and 2. *J. Physiol.*, **537**, 747–761.
Hoenderop,J.G., Dardenne,O., Van Abel,M., Van Der Kemp,A.W., Van Os,C.H., St-Arnaud,R. and Bindels,R.J. (2002a) Modulation of renal $Ca^{2+}$ transport protein genes by dietary $Ca^{2+}$ and 1,25-dihydroxyvitamin $D_3$ in 25-hydroxyvitamin $D_3$-1α-hydroxylase knockout mice. *FASEB J.*, **16**, 1398–1406.
Hoenderop,J.G., Nilius,B. and Bindels,R.J. (2002b) Molecular mechanism of $Ca^{2+}$ reabsorption in the distal nephron. *Annu. Rev. Physiol.*, **64**, 529–549.
Hoenderop,J.G., Voets,T., Hoefs,S., Weidema,A.F., Prenen,J., Nilius,B. and Bindels,R.J. (2003) Homo- and heterotetrameric architecture of the epithelial $Ca^{2+}$ channels, TRPV5 and TRPV6. *EMBO J.*, **22**, 776–785.
Hoffman,C.S. and Winston,F. (1987) A ten-minute DNA preparation from yeast efficiently releases autonomous plasmids for transformation of *Escherichia coli*. *Gene*, **57**, 267–272.
Janssen,S.W., Hoenderop,J.G., Hermus,A.R., Sweep,F.C., Martens,G.J. and Bindels,R.J. (2002) Expression of the novel epithelial $Ca^{2+}$ channel ECaC1 in rat pancreatic islets. *J. Histochem. Cytochem.*, **50**, 789–798.
Kaczan-Bourgois,D., Salles,J.P., Hullin,F., Fauvel,J., Moisand,A., Duga-Neulat,I., Berrebi,A., Campistron,G. and Chap,H. (1996) Increased content of annexin II (p36) and p11 in human placenta brush-border membrane vesicles during syncytiotrophoblast maturation and differentiation. *Placenta*, **17**, 669–676.
Krieg,P.A. and Melton,D.A. (1984) Functional messenger RNAs are produced by SP6 *in vitro* transcription of cloned cDNAs. *Nucleic Acids Res.*, **12**, 7057–7070.
Li,H.S. and Montell,C. (2000) TRP and the PDZ protein, INAD, form the core complex required for retention of the signalplex in *Drosophila* photoreceptor cells. *J. Cell Biol.*, **150**, 1411–1422.
Liedtke,W., Choe,Y., Marti-Renom,M.A., Bell,A.M., Denis,C.S., Sali,A., Hudspeth,A.J., Friedman,J.M. and Heller,S. (2000) Vanilloid receptor-related osmotically activated channel (VR-OAC), a candidate vertebrate osmoreceptor. *Cell*, **103**, 525–535.
Loffing,J., Loffing-Cueni,D., Valderrabano,V., Klausli,L., Hebert,S.C., Rossier,B.C., Hoenderop,J.G., Bindels,R.J. and Kaissling,B. (2001) Distribution of transcellular calcium and sodium transport pathways along mouse distal nephron. *Am. J. Physiol. Renal Physiol.*, **281**, F1021–F1027.
Massey-Harroche,D., Mayran,N. and Maroux,S. (1998) Polarized localizations of annexins I, II, VI and XIII in epithelial cells of intestinal, hepatic and pancreatic tissues. *J. Cell Sci.*, **111**, 3007–3015.
Menaa,C., Devlin,R.D., Reddy,S.V., Gazitt,Y., Choi,S.J. and Roodman,G.D. (1999) Annexin II increases osteoclast formation by stimulating the proliferation of osteoclast precursors in human marrow cultures. *J. Clin. Invest.*, **103**, 1605–1613.
Montell,C., Birnbaumer,L. and Flockerzi,V. (2002a) The TRP channels, a remarkably functional family. *Cell*, **108**, 595–598.
Montell,C. *et al*. (2002b) A unified nomenclature for the superfamily of TRP cation channels. *Mol. Cell*, **9**, 229–231.
Nilius,B., Gerke,V., Prenen,J., Szucs,G., Heinke,S., Weber,K. and Droogmans,G. (1996) Annexin II modulates volume-activated chloride currents in vascular endothelial cells. *J. Biol. Chem.*, **271**, 30631–30636.
Nilius,B., Prenen,J., Vennekens,R., Hoenderop,J.G., Bindels,R.J. and Droogmans,G. (2001) Modulation of the epithelial calcium channel, ECaC, by intracellular $Ca^{2+}$. *Cell Calcium*, **29**, 417–428.
Nilius,B., Prenen,J., Hoenderop,J.G., Vennekens,R., Hoefs,S., Weidema,A.F., Droogmans,G. and Bindels,R.J. (2002) Fast and slow inactivation kinetics of the $Ca^{2+}$ channels ECaC1 and ECaC2 (TRPV5 and 6): role of the intracellular loop located between transmembrane segment 2 and 3. *J. Biol. Chem.*, **277**, 30852–30858.
Okuse,K., Malik-Hall,M., Baker,M.D., Poon,W.Y., Kong,H., Chao,M.V. and Wood,J.N. (2002) Annexin II light chain regulates sensory neuron-specific sodium channel expression. *Nature*, **417**, 653–656.
Peng,J.B., Chen,X.Z., Berger,U.V., Vassilev,P.M., Tsukaguchi,H., Brown,E.M. and Hediger,M.A. (1999) Molecular cloning and characterization of a channel-like transporter mediating intestinal calcium absorption. *J. Biol. Chem.*, **274**, 22739–22746.
Puisieux,A., Ji,J. and Ozturk,M. (1996) Annexin II up-regulates cellular levels of p11 protein by a post-translational mechanisms. *Biochem. J.*, **313**, 51–55.
Rety,S., Sopkova,J., Renouard,M., Osterloh,D., Gerke,V., Tabaries,S., Russo-Marie,F. and Lewit-Bentley,A. (1999) The crystal structure of a complex of p11 with the annexin II N-terminal peptide. *Nat. Struct. Biol.*, **6**, 89–95.
Songyang,Z., *et al*. (1997) Recognition of unique carboxyl-terminal motifs by distinct PDZ domains. *Science*, **275**, 73–77.
Steinmeyer,K., Schwappach,B., Bens,M., Vandewalle,A. and Jentsch,T.J. (1995) Cloning and functional expression of rat CLC-5, a chloride channel related to kidney disease. *J. Biol. Chem.*, **270**, 31172–31177.
Thiel,C., Osborn,M. and Gerke,V. (1992) The tight association of the tyrosine kinase substrate annexin II with the submembranous cytoskeleton depends on intact p11- and $Ca^{2+}$-binding sites. *J. Cell Sci.*, **103**, 733–742.
Van Abel,M., Hoenderop,J.G., Dardenne,O., St Arnaud,R., Van Os,C.H., Van Leeuwen,H.J. and Bindels,R.J. (2002) 1,25-dihydroxyvitamin $D_3$-independent stimulatory effect of estrogen on the expression of ECaC1 in the kidney. *J. Am. Soc. Nephrol.*, **13**, 2102–2109.
Van Cromphaut,S.J. *et al*. (2001) Duodenal calcium absorption in vitamin D receptor-knockout mice: functional and molecular aspects. *Proc. Natl Acad. Sci. USA*, **98**, 13324–13329.
Vennekens,R., Hoenderop,J.G., Prenen,J., Stuiver,M., Willems,P.H., Droogmans,G., Nilius,B. and Bindels,R.J. (2000) Permeation and gating properties of the novel epithelial $Ca^{2+}$ channel. *J. Biol. Chem.*, **275**, 3963–3969.
Vojtek,A.B., Hollenberg,S.M. and Cooper,J.A. (1993) Mammalian Ras interacts directly with the serine/threonine kinase Raf. *Cell*, **74**, 205–214.
Wissenbach,U. *et al*. (2001) Expression of CaT-like, a novel calcium-selective channel, correlates with the malignancy of prostate cancer. *J. Biol. Chem.*, **276**, 19461–19468.
Zobiack,N., Gerke,V. and Rescher,U. (2001) Complex formation and submembranous localization of annexin 2 and S100A10 in live HepG2 cells. *FEBS Lett.*, **500**, 137–140.

*Received October 16, 2002; revised February 7, 2003; accepted February 14, 2003*